TagFree: Passive Object Differentiation via Physical Layer Radiometric Signatures

Yongpan Zou[§], Yuxi Wang[§], Shufeng Ye[†], Kaishun Wu[†] and Lionel M. Ni[‡]
[§]Department of Computer Science and Engineering, Hong Kong University of Science and Technology
[†]College of Computer Science and Software Engineering, Shenzhen University
[‡]Department of Computer and Information Science, University of Macau
{yzouad, katywang}@cse.ust.hk, wo2lifeng@gmail.com, wu@szu.edu.cn, ni@umac.mo

***Abstract*—Object differentiation plays a vital role in our daily life and such systems are widely deployed with RFID tags or bar codes attached on goods. In certain scenarios, however, attaching tags to objects may be impractical due to cost and protection issues. In this paper, we propose TagFree, a novel object differentiation scheme without attaching tags. Instead of relying on external tags, we exploit the inherent radiometric properties of different objects as their signatures. To improve the robustness and efficiency of TagFree, we empirically determine a spatial *safe zone* and harness *successive cancellation* to distinguish multiple objects simultaneously. We prototype TagFree on commercial WiFi infrastructure and evaluate its performance in various indoor scenarios. Experimental results demonstrate that TagFree achieves single object distinguishing accuracy of 96% measured at the same location, and over 80% within the safe zone range of up to 3m along a 7m link. TagFree can also differentiate up to 3 objects with acceptable accuracy.**

I. Introduction

Object distinction plays a central role in supply-chain management, asset tracking, automatic tolling, security access control, etc. Mainstream distinction schemes include bar code and RFID systems, where a unique tag is attached to each object beforehand, and a reader distinguishes one specific object by scanning the information stored in the tag [1], [2]. However, tag-attached objects may sometimes be impractical. For instance, it would impair the overall appearance of artworks such as paintings and sculptures by attaching tags, while ancient crafts and fossils are too fragile and precious to be pasted tags on. Although it is common to label such items by placing tags around them, it incurs extra care when moving these items to avoid tag missing. It is therefore highly desirable to leverage *intrinsic* characteristics of objects, rather than *external* tags, to identify objects *passively* and *unobtrusively*. While radio frequency tomography or visual recognition can serve for this purpose, they often involve dedicated infrastructure or sophisticated computation, thus impeding pervasive and real-time adoption. In this paper, we ask the question: *can we exploit the ubiquitous WLAN signals such as WiFi to identify objects without attaching tags?* If this comes true, many amazing applications can be accomplished. For another example, it can be potentially applied to detect whether a passenger carries common dangerous goods in security check in occasions such as airports. With this unnoticeable check, we envision that it reduces the equipment cost and labor resources.

The past decade has witnessed vast innovations in WLAN device-free applications ranging from motion detection [3], [4], [5], [6], indoor localization [7], [8], [9], to gesture recognition [10], [11], where the target (often a person) carries no wireless enabled devices or tags. The physical underpinning is that target presence or motion affects wireless propagation, and thus received signals. These systems mostly target at *humans*, and assume *identical* radiometric properties of individuals. Therefore they correlate different received signals to different locations or motion patterns. For object distinction, in contrast, we exploit the fact that objects of different material, shapes and sizes exhibit distinctive reflection, refraction and scattering properties [12], and explore to utilize radio signal patterns as signatures for different objects.

Leveraging radiometric characteristics as an object's signature, however, entails numerous challenges. Although textbooks offer various tables enumerating radiometric parameters of typical material and objects [12], it is non-trivial to build precise radiometric models for all objects of various material, shapes and sizes. A more practical approach is to measure and store the radiometric signatures of objects on demand, with off-the-shelf infrastructure. Commercial WiFi devices, unfortunately, provide only single-valued MAC layer signal strength, which is too coarse-grained to extract distinctive radiometric signatures of different objects. We take advantage of the recently exposed fine-grained PHY layer information available on commodity WiFi network cards with modified firmware [13], and strive to extract distinctive radiometric features harnessing both frequency and spatial diversity.

However, radio propagation in typical indoor environments tends to be complex and site-specific. Since the received signals involve both the impact of the target object and background environment (e.g., multipaths induced by walls and furniture), it is possible for the radiometric signatures of one object measured at two locations to differ, thus degrading distinguishing accuracy. It also poses cumbersome overhead to measure and store the signatures for each object at every location. To make it robust to environmental interference and reduce the efforts to build large site-specific signature database, we empirically identify a *safe zone*, within which the target object, rather than site-specific environments, dominates the radiometric impact on received signals.

The ability to identify multiple objects simultaneously is crucial for fast and energy-efficient applications. To accomplish this, we utilize *successive cancellation* techniques [15][16] to identify multiple objects at one time. More specifically, we iteratively search for the best matched radiometric signature in the pre-stored database and subtract its impact from the current received signal signature, until no more objects can be identified. To cope with collaborate fading where impacts of multiple objects superpose nonlinearly [16], we introduce *correlation coefficient*. By training signal data of single object, we adjust the correlation coefficient to cancel out

978-1-5090-4327-9/17/$31.00 ©2017 IEEE

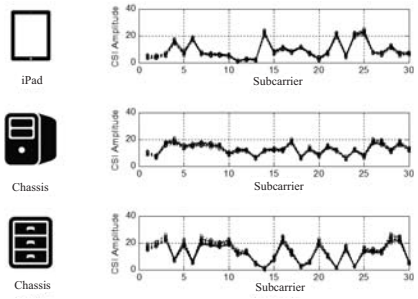

Fig. 1. CSI from 20 packets of 3 different objects measured at the same location along the same link.

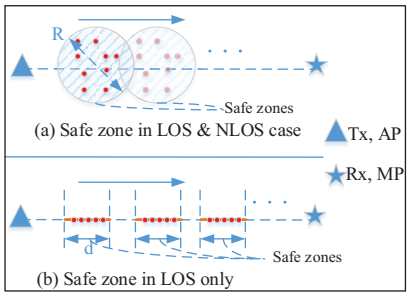

Fig. 2. The pictorial illustration of the concept of safe zone in 1D and 2D scenarios.

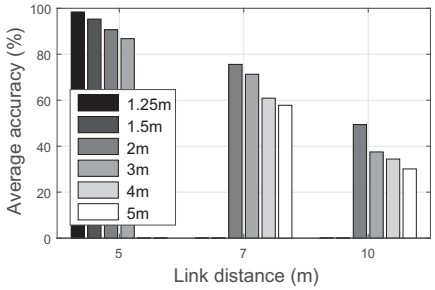

Fig. 3. Average distinguishing accuracy with different object distances and link distances.

purer influence of objects already identified from the mixed signal signature of multiple objects, thus achieving higher accuracy.

Following the above the ideas, we design, implement and evaluate TagFree, a device-free object differentiation system via PHY layer radiometric signature with commodity WiFi infrastructure. Extensive evaluations in two typical indoor scenarios demonstrate that TagFree can achieve up to 96% distinguishing accuracy for each object placed at the same location, and 80% for 3m *Safe Zone* range along a 7m link. Further, TagFree is able to distinguish up to 3 objects concurrently with *Successive Cancellation*. In a nutshell, the main contributions can be concluded as follows:

- We exploit the intrinsic radiometric characteristics of heterogeneous objects to differentiate different objects in a device-free manner. To the best of our knowledge, this is the first effort in distinguishing objects via PHY layer information on commodity WLAN infrastructure.
- We empirically determine a spatial *safe zone*, where the impact of objects, rather than locations, dominates in determining the received signal properties, making our object differentiation scheme robust to environmental interference.
- We propose to differentiate multiple objects simultaneously via *Successive Cancellation*, which makes TagFree differentiate up to 3 objects at a time with acceptable accuracy and dramatically boosts object distinction efficiency.

In the rest of this paper, we first provide a preliminary introduction on PHY layer information as well as the key measurements and observations in Section II, followed by detailed design of TagFree in Section III. Section IV presents the implementation and comprehensive performance evaluation of TagFree in typical indoor scenarios. We summarize related work in Section VI and conclude in Section VII.

II. Background and Measurements

This section demonstrates the feasibility of distinguishing objects via radiometric signatures through measurements. We start with a brief introduction on PHY layer CSI, followed by the essential properties that CSI must hold as radiometric signatures.

A. Channel State Information

In typical cluttered indoor environments, signals often propagate to the receiver via multiple paths. Such multipath effect creates varying path loss across frequencies, known as *frequency diversity* [12]. Conventional MAC layer RSSI provides only a single-valued signal strength indicator. Modern multi-carrier radio such as OFDM measures frequency diversity at the granularity of subcarrier, and stores the information in the form of Channel State Information (CSI). Each CSI depicts the amplitude and phase of a subcarrier:

$$H(f_k) = \|H(f_k)\|e^{j\sin(\angle H)} \quad (1)$$

where $H(f_k)$ is the CSI at the subcarrier with central frequency of f_k, and $\angle H$ denotes its phase. Leveraging the off-the-shelf Intel 5300 network card with a publicly available driver [13], a group of CSIs $H(f)$ of $K = 30$ subcarriers are exported to upper layers.

$$H(f) = [H(f_1), H(f_2), \ldots, H(f_K)] \quad (2)$$

As an illustration, Fig. 1 plots the CSIs measured along the same link with three different objects (an iPad, a chassis and a cabinet) placed at the same location.

Recent WLAN standards (e.g. 802.11n/ac) also exploit MIMO techniques to boost capacity via *spatial diversity*. We thus involve spatial diversity to further enrich channel measurements. Given M receiver antennas and N transmitter antennas, we obtain an $M \times N$ matrix of CSIs $\{H_{mn}(f)\}_{M\times N}$, where each element $H_{mn}(f)$ is defined as Equation 2. In a nutshell, PHY layer CSI portrays finer-grained spectral structure of wireless channels. Spatial diversity provided by multiple antennas further expands the dimensions of channel measurements. As a result, TagFree utilizes the rich feature space of CSI to identify different objects with only a single AP. However, to identify objects robustly and efficiently, two issues are of particular interest in TagFree.

- CSI reflects both the impact of the target object along the link and background environment. It is unclear how these site-specific uncertainties would affect the CSI based radiometric signatures of different objects.
- Simultaneous object identification would dramatically improve identification efficiency. Yet it is unknown whether the impact of multiple closely placed objects is separable.

To study these issues, we design measurements as follows.

978-1-5090-4327-9/17/$31.00 ©2017 IEEE

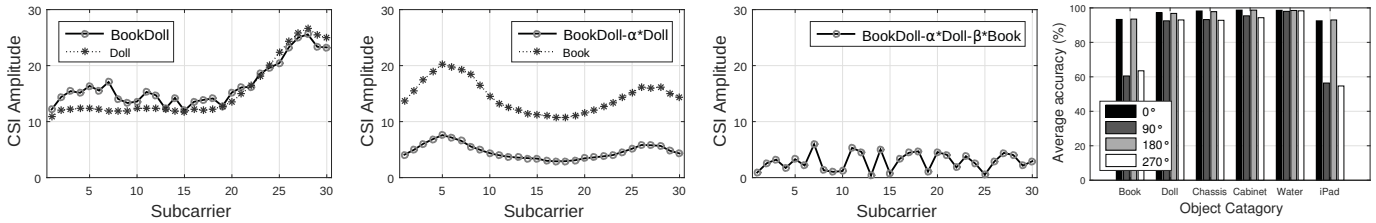

(a) the superposed measurements of a doll and a book

(b) the residual measurement after the first cancellation operation

(c) the residual measurement after the second cancellation operation

Fig. 4. The illustration of recognizing multiple objects simultaneously with successive cancellation techniques.

Fig. 5. The results of differentiating objects in different orientations.

B. Measurements and Observations

This section provides preliminary measurements and observations in two aspects, i.e., identifying a *Safe Zone* and exploring *Multi-Signature Separation*, respectively.

1) Safe Zone: Due to site-specific propagation, the CSI based signatures of the same object may differ when measured at different locations, leading to erroneous classification. To quantify the impact of such environmental interference, we empirically define a *Safe Zone* which is a certain region with fixed size along the LOS (Line-Of-Sight) as shown in Fig. 2. Within a safe zone, object diversity, rather than site-specific propagation, dominates the impact on the channel and radiometric signatures of a same object at different locations share much similarity. Thus, even though the signatures of an object are collected at different locations in a safe zone, it can be recognized with high accuracy. Fig. 2 gives a pictorial illustration of *Safe Zone*.

Measurement Setup: We deploy one AP (Access Point) and one MP (Monitoring Point) in a typical lobby environment, and test 6 categories of objects: a book (paper, 260×185mm), an iPad (magnalium, 240×169.5×7.5mm), a cotton doll (plush, D200mm×500mm), a desktop chassis (iron, 150×400×100mm), a wooden cabinet (wood, 300×300×300mm), and a barrel of water (plastic&water D280mm×400mm). The reason why we choose these objects is based on the following considerations: 1) Objects should differ in material or/and size. Otherwise, it is not feasible to differentiate different objects via RF signature; 2) Objects should be common in our daily life. In this paper, we mainly focus on LOS condition and leave the thorough scrutiny on NLOS for future work. Consequently, a safe zone can be reduced to a 1D distance interval along the LOS as shown in Fig. 2(b). We place each object at various positions along the LOS link and collect CSI data from the MP. We pick data measured at one location for training, while those at another location for testing. Since a safe zone in this case is one-dimensional, we focus on two factors that potentially affect the boundary of safe zone: (1) *link distance*: the distance between the AP and the MP. We measure link distance of 5m, 7m and 10m, respectively. (2) *object distance*: the distance between training data and testing data. We evaluate the object differentiation performance with object distance of 1.25m, 1.5m, 2m, 3m, and 4m, respectively.

Observations: After collecting the CSI data, we extract proper features (detailed in Section III-B) and evaluate the distinguishing accuracy of the above 6 objects measured at different locations. Fig. 3 illustrates the overall distinguishing performance[1]. In general, the overall accuracy degrades with both link distance and object distance. However, with a 5m link and objects placed 3m away, the overall accuracy retains above 85%, and even with object distance of 4m along a 7m link, the distinguishing accuracy is still significantly higher than a random guess. We make two observations herein: i) Link distance deteriorates object differentiation performance more severely than object distance due to more environmental uncertainties involved along signal propagation; ii) Object accuracy dramatically decreases on long links even with short object distance. Therefore, we define *safe zone* of common objects as a range of at most 3-4m along a 7m link. Additionally, when the link distance is less than 5m, the safe zone is highly reliable. We defer comprehensive evaluations of safe zone and discussions on its scalability to Section IV-B.

2) Multi-Signature Separation: To distinguish multiple objects *simultaneously*, we try to resolve the radiometric impact of one dominant object from that of a mixture of objects, subtract it, and continue to decode the impact of the second dominant object from the remaining, until no object can be detected. As a preliminary verification this idea, we conduct the following measurements.

Measurement Setup: We deploy one AP and one MP separated by 3m in a laboratory, which guarantees the impact of objects dominates over environmental uncertainties as discussed in Section II-B1. As a primary study, we test the combination of a large cotton doll and a book. We first place the doll and the book together at the middle point of the link, and then put each of them separately at the same location.

Observations: For ease of illustration, we only demonstrate the CSIs from one channel out of the $3 \times 3 = 9$ in our MIMO system. Fig. 4(a) plots the mixed radiometric signature of the doll and the book (labeled as $BookDoll$) and the signature of the doll. Due to the relatively large size of the doll, the impact of the doll dominates the superposed radiometric impact and consequently, the mixed signature and the signature of the doll roughly share a similar shape over frequency. We are thus able to compare the similarity between the mixed signature and those of each single object, and match that of the doll. After that, we cancel the impact of the doll from the mixed signature and search for the best match between the residual signature and the signatures of individual objects.

One crucial observation is that we cannot subtract the

[1]It is noted that some cases such as 1.25m, 1.5m and 2m object distances for 7m and 10m links are not tested as demonstrated in IV-B3, the corresponding results are not shown in the figure which does not mean they are equal to zeros.

978-1-5090-4327-9/17/$31.00 ©2017 IEEE

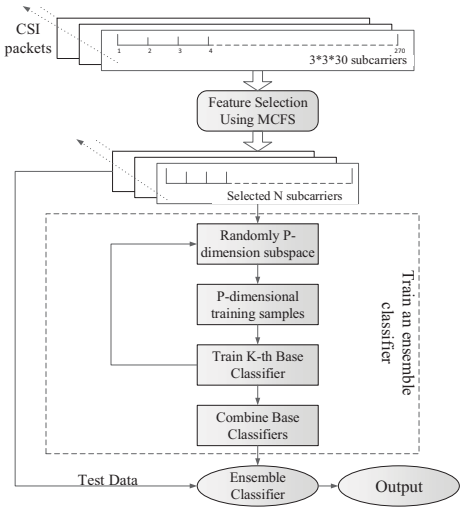

Fig. 6. Data processing flow of TagFree.

impact of the doll directly due to correlated fading [16]. Therefore we first multiply the signature of the doll by a *correlation coefficient* α before subtracting it from the superposed signature. This parameter represents the weight of radiometric signature of a certain object in the composition of multiple objects. The rationale of introducing *correlation coefficient* lies in the fact that the composite radiometric signature of multiple objects is composed of weighted signature of each single object due to the channel fading effect. Fig. 4(b) depicts the residual signature $BookDoll - \alpha * Doll$ as well as the signature of the book. Since the residual and the book signature again resemble in shape, we would be able to match the residue with the book signature, which is previously buried in the impact of the doll. To check whether there are other objects remaining, we also cancel the impact of the book in the same way, yet with a book related correlation coefficient β. As shown in Fig. 4(c), as we fail to find any signature match for the residue $BookDoll - \alpha * Doll - \beta * Book$, the process terminates and thus we distinguish a doll and a book simultaneously by only one mixed measurement. The measurements demonstrate two key insights: i) Within the safe zone, the superposed impact of multiple objects can be separated and resolved by iteratively cancelling the impact of the dominant object; ii) Due to the correlated shading effect [16], we need to identify an object-specific correlation coefficient when subtracting the impact of one object from the mixed signature. As a result, we elaborate our iterative object differentiation scheme based on these insights in Section III-D and evaluate its performance for multi-object identification in Section IV-C.

In a nutshell, the above measurements and observations validate the feasibility of CSI as robust and effective radiometric signatures to distinguish objects. The subsequent sections strive to extract informative and representative features from CSI, and design a systematic scheme for object differentiation.

III. TagFree Design

In this section, we detail our design of TagFree by first providing an overview and then detailed descriptions on the main modules.

A. Overview

TagFree builds upon off-the-shelf WLAN infrastructure, a laptop equipped with Intel 5300 network card as MP, and a wireless router as AP. TagFree works in two stages: *training* and *operating*. During the *training* stage, different objects are placed along the AP-MP link to build up a signature database for all target objects. For each object, the MP receives packets from the AP and extracts CSI from each packet. Representative features are then extracted from the CSI data and stored for each object as its radiometric signature in the database stored either in the MP or uploaded to a central server. The training data is then utilized to train an ensemble classifier. During the *operating* stage, when multiple objects are placed within a safe zone, the MP measures the CSI data from the received packets from the AP, extracts features, and iteratively retrieves the object with the best match signature in the database, cancels its impact, and performs another round of signature matching using the residue, until no object matches the residue. Fig. 6 outlines the data processing flow of TagFree, and in what follows, we mainly elaborate on feature extraction, training and classification, as well as the iterative signature matching scheme, respectively.

B. Feature Extraction and Signature Representation

As discussed in Section II-A, a set of 30 CSI is exposed for each channel, each representing the amplitude and phase of an OFDM subcarrier. Together with the 3×3 MIMO system, we obtain a 270-dimension vector from each received packet. To avoid the well-known "dimensionality curse", and mitigate the irrelevant environmental interference, we exploit a Multi-Cluster/Class Feature Selection (MCFS) scheme [17]. Compared with other feature selection methods, MCFS can produce an optimal feature subset by considering possible correlations between different features, which better conforms to the characteristics of the dataset. Indeed, the input amplitudes within the 270-dimension CSI vector are correlated in two aspects: 1) the dimensions corresponding to the same channel are correlated because they experience similar radio propagation environment; and 2) the dimensions corresponding to neighbor subcarriers are correlated as they are close in frequency. Therefore, by harnessing the MCFS feature selection scheme, we efficiently reduce the dimensions of the feature space, and retain the distinctive radiometric impact of objects at the same time. In addition, feature selection also improves prediction performance and reduces computational cost [18].

For a set of N CSI data points $P = [p_1, p_2, ...p_N]$ where $p_i \in \mathbb{R}^M$, and $M = 270$ in our case, MCFS works as follows. Firstly, a m-nearest neighbor graph is constructed from the original dataset P. More concretely, a graph of N vertices is constructed, where each vertex corresponds to a CSI data point p_i. For each p_i, once its m nearest neighbors are determined, weighted edges are assigned between p_i and each of its neighbors, respectively. We define the weight matrix W for the edge connecting node i and node j as:

$$W_{i,j} = e^{-\frac{\|p_i - p_j\|^2}{\varepsilon}} \tag{3}$$

where ϵ is a constant adjusting the weight assignment. Secondly, MCFS solves the following generalized eigen-problem:

$$Lv = \lambda Av \tag{4}$$

978-1-5090-4327-9/17/$31.00 ©2017 IEEE

where A is a diagonal matrix and $A_{ii} = \sum_j W_{ij}$. The graph Laplacian L is defined as $L = A - W$. And V is defined as $V = [v_1, v_2, ...v_K]$, in which all the v_k are the eigenvectors of Equation 4 with respect to the smallest eigenvalue. Thirdly, given v_k, a column of V, MCFS searches for a relevant feature subset by minimizing fitting errors:

$$\min_{\alpha_k} \|v_k - P^T \alpha_k\|^2 + \gamma|\alpha_k| \tag{5}$$

where α_k is a M-dimensional vector and $|\alpha_k| = \sum_{j=1}^{M} |\alpha_{k,j}|$ represents the L_1-norm of α_k. Finally, for every feature j, MCFS defines the MCFS score for the feature as:

$$Score(j) = \max_k |\alpha_{k,j}| \tag{6}$$

where $\alpha_{k,j}$ is the j-th element of vector α_k and all the features are sorted by their MCFS scores in descending order and the top d features are chosen as the selected features. In our implementation, we empirically select the top 30 features as signatures for different objects, and remove the redundant and irrelevant features in the original CSI data vector.

C. Training and Classification

Since indoor environments often involve multipath propagation and irrelevant dynamics, e.g., occasional pedestrian passing-by, the received CSI measurements sightly fluctuate. Due to the high dimensionality of CSI data even after feature selection, though, even small signal perturbation might lead to a single classifier with poorly estimated parameters [19]. Therefore, we construct an ensemble classifier via ensemble learning methods to deal with the noisy high dimensional CSI data. Bagging, Boost, and Random Subspace Method (RSM) are classical schemes for ensemble learning and we choose RSM for the following reasons. On one hand, RSM modifies the training dataset in the feature space rather than the original sample space [20]. On the other hand, RSM outperforms bagging and boost schemes in general [19]. To obtain better object differentiation performance, we explore a more sophisticated scheme: Spectral Regression Discriminant Analysis (SRDA) [21] which is based on the popular Linear Discriminant Analysis (LDA) yet mitigates computational redundancy.

D. Iterative Object Identification

As shown in Section II-B2, TagFree explores to distinguish multiple objects simultaneously from their mixed radiometric signatures to improve differentiation efficiency. To achieve such capability, however, is non-trivial. It is shown in [16] that the impact of multiple objects on received signals is non-linear. Therefore it is infeasible to remove the impact of one object from the mixed signatures by subtracting the corresponding signature stored in the database. The non-linear impact also leads to the possibility that the impact of one group of objects resembles that of another group. Thus it is more challenging to figure out the correct object combination.

To address the above issues, we propose a multi-signature separation scheme leveraging *successive cancellation*. As described in the illustrative example in Section II-B2, we iteratively process two steps:

- **Step 1:** Retrieve in the signature database and return the one that best matches the current residual (mixed) signature.
- **Step 2:** Remove the impact of the matched signature by deducing it from the current mixed signature. To cope with the non-linear impact, the matched signature is multiplied by a *correlation coefficient* from a pre-measured correlation coefficient matrix before subtracting it from the mixed signature.

The process terminates when no more matching can be found in the residual signature, i.e. a matching failure. We empirically define a matching failure as the case when the maximum correlation between the test signature and all the signatures stored in the database is no more than 50%. To determine the correlation coefficient matrix C, we resort to the following minimization problem:

$$\min \sum_{i=1}^{M} \frac{\|C_{i,j} \times H_{i,j} - \mathbb{H}_i\|^2}{N_i} \tag{7}$$
$$\text{Subject to } \forall\, \mathbb{H}_i \neq 0 \ , \ C_{i,j} \neq 0$$

where $C_{i,j}$ and $H_{i,j}$ denote the correlation coefficient and the CSI signature of object j in link i, respectively. i is the index of links and $1 \leq i \leq M$, where M is the number of links and $M = 3 \times 3 = 9$ in our case. N_i stands for the quantity of subcarriers that are chosen into the signature in the i^{th} link, which varies from 0 to 30. $\mathbb{H}_i$ refers to the current mixed CSI signature of multiple objects in link i.

IV. Performance

This section presents the implementation and performance evaluation of TagFree in different scenarios.

A. Experimental Setup

1) Implementation: We implement the proposed TagFree system with a TP-LINK TL-WDR4300 wireless router as the transmitter, and a 3.20GHz Intel(R) Pentium 4 CPU 2GB RAM desktop equipped with Intel 5300 NIC as the receiver. The transmitter possesses 3 detectable antennas and operates in IEEE 802.11n AP mode at 5GHz. The receiver has 3 working antennas and the firmware is modified as in [13] to report CSI to upper layers. During the measurement campaign, the receiver continuously pings packets from the AP at the rate of 100 packets per second and we collect CSIs for 1 minute during each measurement. The collected CSIs are then stored and processed at the receiver to differentiate different objects.

2) Experimental Scenarios: We conduct the measurement campaign in 3 typical indoor environments in the campus and test 6 objects of different materials, shapes and sizes, including a book, an iPad, a cotton doll, a desktop chassis, a wooden cabinet, and a barrel of water. In each scenario, we first collect data when no object is present along the link, and then place the testing objects at different locations along the link. The detailed experimental scenarios are as follows.

- **Chamber.** We first measure CSIs of the 6 objects in a 3m×4m chamber to collect radiometric signatures without multipath and external interference (Fig. 7a). Each object is placed in the midpoint of a 2m link.

978-1-5090-4327-9/17/$31.00 ©2017 IEEE

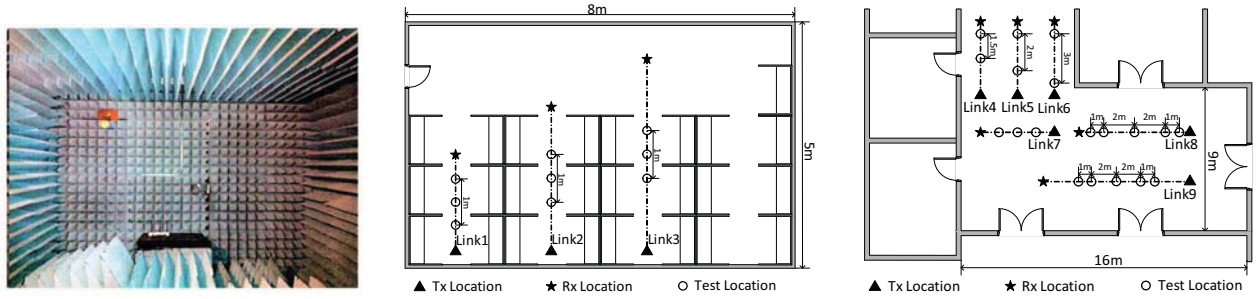

(a) Chamber (b) Laboratory (c) Lobby

Fig. 7. Illustration of experimental scenarios: (a) Chamber environment; (b) Relatively short test links in a typical multipath-rich research laboratory; (c) Test links in a relatively open lobby area with long links.

- **Laboratory.** We then deploy TagFree in a multipath-rich 5m×8m laboratory where there exist desks, chairs, desktops, humans and some other objects common in a lab. Moreover, there also exists RF interference in the lab. In this scenario, we test relatively short link distance of 2m to 4m (Link 1 to Link 3 in Fig. 7b). For each link, we collect CSIs for multiple objects. Specifically, we test combinations of 2, 3, and 4 objects. For each combination, we fix the locations of the objects, and measure CSIs for both the combination and each single object.
- **Lobby.** Finally, we conduct measurements in a relatively open lobby area covering 9m×16m. Compared with the lab, the lobby is empty without any objects except RF inference. As a result, the multipath effect in the lobby is relatively minute. As illustrated in Fig. 7c, we collect CSIs for the 6 test objects with relatively long link distance of 5m (Link 4 to Link 7), 7m (Link 8) and 10m (Link 9), respectively.

It is noted that without special declaration, in Lab and Lobby scenarios, there are two persons walking around the experimental setup with a distance of 2m away from the AP-MP link in each set of experiments, in order to evaluate the robustness of TagFree in realistic settings.

B. Performance of Single Object Differentiation

This section presents the performance of single object differentiation with different object orientations, object distances, link distances and number of training samples, as well as a brief discussion on the scalability of TagFree to long link distance scenarios.

1) Impact of Different Orientations: Since objects can be placed in various orientations at a position, we evaluate the impact of orientation on distinguishing objects by spinning them every ninety degrees around their vertical axises at a same location. Specially, the objects are placed in the middle point of a AP-MP link with a moderate length (5m) in the lobby as shown in Fig. 7c. As shown in Fig. 5, the accuracy of distinguishing objects varies with object orientations, especially for 'Book' and 'iPad'. For other objects, the orientation has minor influence on their differentiation accuracies. The reason is that there is little cylindrical symmetry around the vertical axis for 'Book' and 'iPad', while other objects have approximate cylindrical symmetry around their vertical axises. As a result, when 'Book' and 'iPad' are placed in different orientations, their accuracies varies much from about 90% to 60%. For other objects, due to their approximate cylindrical symmetry, the accuracies can maintain relatively stable with a variation of about 2%. As a result, for 'Book' and 'iPad', we only test the sole case of 0° orientation and consider the average performance in different orientations for other objects in the following experiments. Discussion about impact of orientation is detailed in Section V.

2) Performance at the Same Location: We first evaluate the effectiveness of TagFree when the training data and the testing data are measured from the same position, i.e. with object distance of zero. Under such a condition, we place objects at different locations with equal interval along the link, obtain the distinguishing results in each location and finally average them as the overall performance in the case of same-location distinguishing. For each link, the number of locations equals to the link length. Fig. 8 demonstrates the overall confusion matrices of the 6 objects described in Section IV-A2 with link distance of 5m, 7m and 10m, respectively (Fig. 7c). As shown in Fig. 8a, the average distinguishing accuracy of single object distinction of all the 6 objects is above 96% for the 5m link (false positive rate, FPR=0.8%; false negative rate, FNR=3%), and the differentiation performance only experiences a slight degradation for the 7m link, with average distinguishing accuracy still above 90% (FPR=1.8%; FNR=9%) in Fig. 8b. However, the average distinguishing accuracy drops moderately to about 72% (FPR=5.8%; FNR=29%) for the 10m link in Fig. 8c partially due to more environmental uncertainties along long links.

Moreover, as we can see from the figure, the distinguishing accuracy of different objects also varies. For instance, the distinguishing accuracy of book remains high compared with that of the other 5 objects. This is because when the training data and the testing data are measured at the same location, only the size, shape and material of the object will affect the channel. Therefore, due to its comparatively small size and little signal attenuation, the book tends to be more distinguishable than the other objects (e.g. the iPad is of small size but made of metal, while the doll induces less attenuation yet is large in size).

3) Impact of Locations: As discussed in Section II-B, locations affect the performance of TagFree from two aspects: (1) object distance (the physical distance between the location

978-1-5090-4327-9/17/$31.00 ©2017 IEEE

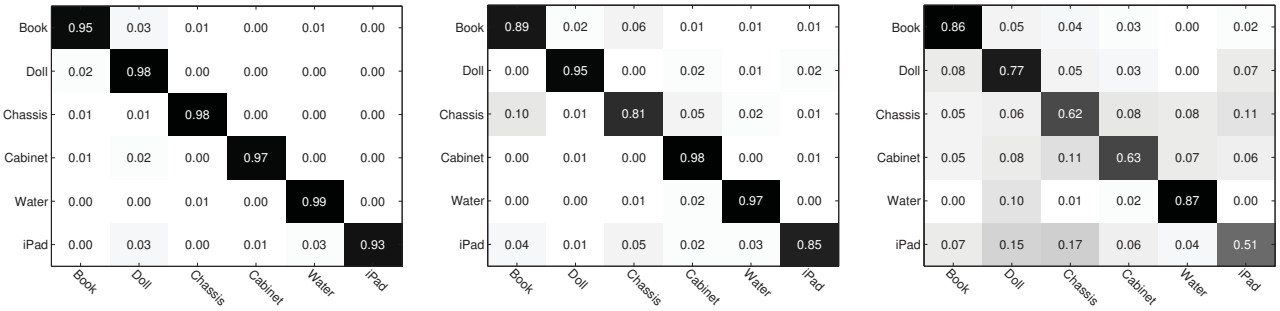

(a) 5m link distance (b) 7m link distance (c) 10m link distance

Fig. 8. Confusion matrices for single object differentiation with object at the same location of link distance of (a) 5m (b) 7m and (c) 10m.

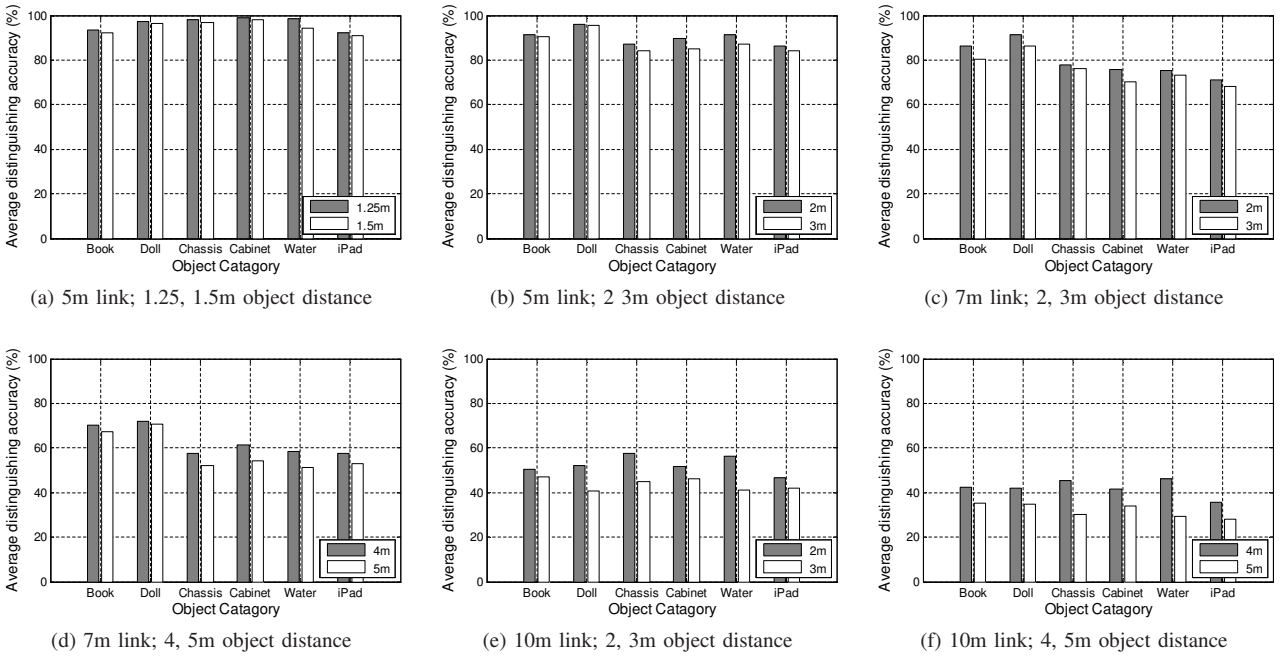

(a) 5m link; 1.25, 1.5m object distance (b) 5m link; 2 3m object distance (c) 7m link; 2, 3m object distance

(d) 7m link; 4, 5m object distance (e) 10m link; 2, 3m object distance (f) 10m link; 4, 5m object distance

Fig. 9. Average distinguishing accuracy with different link distance and object distance: (a)-(b) 5m link; (c)-(d) 7m link; (e)-(f) 10m link.

of the data collected for training and that of the data collected for testing) and (2) link distance (the physical distance between the AP and the MP). The previous subsection focuses on performance with object distance of zero, and we extend to evaluate the performance with object distance up to 5m herein. Fig. 9 plots the average distinguishing accuracy of the 6 objects with various object distance and link distance.

Impact of Object Distance. As shown in Fig. 7c, we evaluate the performance of object distance of 1.25m (Link7), 1.5m (Link4), 2m (Link5) and 3m (Link6) for the 5m link, and 2m, 3m, 4m, and 5m for the 7m and 10m links (Link8 and Link9, respectively), respectively. It is noted that we have tested four combinations of object distances in Link8 and Link9 as shown Fig. 7c. For each link length, we collect data at locations shown in the figure, train the system with data in one location and test its performance with data in another location with a certain object distance away from the training location. As shown in Fig. 9a, the distinguishing accuracy stays above 95% on average when the object distance is within the range of 1.5m on the 5m link, which is almost as high as that of the same location (i.e. object distance of zero). For object distance of 2m and 3m, the distinguishing accuracy is still reasonably high. Although the performance of 3m range is worse than that of 2m range, the performance degradation is modest, with a drop of around 5% for the 5m link (Fig. 9b), 6% for the 7m link (Fig. 9c) and 13% for the 10m link (Fig. 9e), respectively. For longer object distance (e.g. 4m and 5m), the overall accuracy decreases by over 16% for the 7m link and 8% for the 10m link, compared with that of object distance of 2m and 3m for the corresponding link distance. The lower performance degradation for the 10m link is because the change of object distance from 2m (or 3m) to 4m (or 5m) induces less impact compared with the change of link distance from 7 m to 10 m. In summary, the distinguishing accuracy of TagFree remains satisfactory when the object distance is within 1m to 2m, which accords with the preliminary study in Section II-B.

Impact of Link Length. As shown in Fig. 9b and Fig. 9c, the average distinguishing accuracy declines nearly 11% when link distance increases from 5m to 7m. This drop is much more severe than the cases when object distance increases

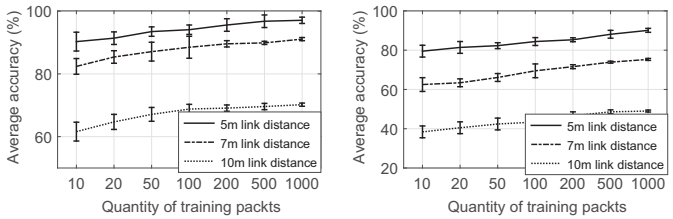

(a) Placing objects at the same location (b) Placing objects in the 1m safe zone

Fig. 10. Impact of training data quantity on average distinguishing accuracy when objects are placed (a) at the same location and (b) within the safe zone.

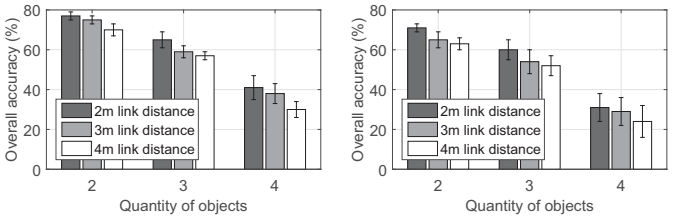

(a) Placing objects at the same location (b) Placing objects in the 1m safe zone

Fig. 11. Overall distinguishing accuracy of multi-object differentiation when the single object's training data and the test multiple objects are placed are placed (a) at the same location and (b) within the safe zone.

an equal amount. Similarly, as shown in Fig. 9c and Fig. 9e, the distinguishing accuracy deteriorates dramatically (with an average decline of 29%) when link distance further increases from 7m to 10m. Especially for the book and the doll, the decrease is almost 34%. The substantial performance degradation is mainly due to severe and uncertain signal attenuation. Thus the impact of objects on received signals is significantly weaker along long links than along short links. In conclusion, compared with object distance, the impact of link length dominates the performance of single object differentiation, and both long object distance and long link distance lead to sharp decline in distinguishing accuracy (Fig. 9d and Fig. 9f).

4) Training Overhead: Intuitively, more training samples contribute to better classifiers and thus higher distinguishing accuracy. And we evaluate this training overhead of TagFree in this subsection. We mainly focus on two scenarios: (1) measurements of the same location and (2) measurements within a 2m safe zone (object distance of 2m). As demonstrated in Fig. 10, the overall distinguishing accuracy rises steadily with more training packets. Yet we only need 100 to 200 packets (corresponding to 1s to 2s) to train a satisfactory classifier. The relatively low training overhead is due to the feature selection scheme of TagFree, which efficiently captures the most representative radiometric features from only a small amount of samples. Comparing Fig. 10a and Fig. 10b, the training overhead is larger for the case of a 2m safe zone than for the case of the same location. For instance, it needs about 1000 training packets for the former case to achieve similar accuracy while 100 packets for the latter case. This is because within the safe zone, more training packets are needed to extract coherent features of objects and eliminate the impact of locations.

5) Scalability of Safe Zone with Long Link Distance: As demonstrated in previous subsections, the differentiation performance is far from satisfactory for link distance more than 10m. A natural question is how to improve distinguishing accuracy for long links. A general design is to exploit multiple link pairs to compensate for the environmental interference induced by long links. For instance, when placing one more link pair perpendicular to the original pair, we expand our measurements by one fold. With more information (largely uncorrelated due to spatial diversity), we can combine more features to enhance differentiation performance. We extend our experimental platform into 2 link pairs that are mutually vertical. For each measurement, we move one pair of AP-MP link simultaneously with the object, so that the object is always on the cross of two LOS paths. According to our measurements, for link distance of no more than 7m , the accuracy improvement is marginal (0.67% on average for 5m and 2.31% for 7m). The reason for this phenomenon might be that the accuracy for a single link pair is already close to the upper bound. Thus more information do not contribute to substantial gain. For the 10m link, in contrast, the accuracy improvement is relatively significant after our 2-link expansion. The average accuracy improvement is 13.47%. More precisely, the accuracy improvement is 9.73% for object distance of 2m, 18.49% for object distance of 3m and 12.19% for object distance of 4m, respectively. Due to current infrastructure limit, however, we leave comprehensive investigation on multi-link fusion in future work.

C. Performance of Multiple Object Differentiation

Similar to the previous subsections, we evaluate the performance of multi-object differentiation in two scenarios: (1) successive cancellation at the same location (i.e., at the midpoint of the link), and (2) successive cancellation within a 1m safe zone range. To avoid the severe impact of long link distance, we mainly evaluate the performance of multi-object differentiation for link distance of 2m to 4m (Link 1-3 in Fig. 7b). To eliminate the impact of multipath propagation, we exploit the data collected in the chamber (Fig. 7a) to calculate the correlation coefficient matrix.

As shown in Fig. 11a, with link distance of 2m to 4m, the average accuracy is 75% and 57% for 2 and 3 objects, respectively. The high distinguishing accuracy indicates that TagFree can easily match the doll or cabinet remove its impact at the first round of cancellation. This is because the size and material of the doll or cabinet make it dominate in the mixed radiometric impact. And with the help of the pre-measured correlation coefficient matrix, we can deal with the non-linear correlated fading of multiple objects and remove the impact of the dominant object more thoroughly than simply subtracting its impact from the mixed signature. However, when it comes to 4 objects, the performance drops sharply, with average accuracy of only about 30% due to interference and noise. For the 1m safe zone range, it becomes even more challenging to distinguish multiple objects. As depicted in Fig. 11b, the average distinguishing rates of 2 objects and 3 objects are above 63% and 52%, respectively. The reasonably high accuracy partially owes to the feature selection procedure in TagFree, which assists to remove redundant information and other interference. More concretely, after feature selection, we remove much of the environmental effects so that the extracted features represent the inherent radiometric impact of the object itself rather than external impact of locations. Since

978-1-5090-4327-9/17/$31.00 ©2017 IEEE

the accuracy of distinguishing more than 4 object is pretty low in both scenarios, it remains unsettled how to improve the scalability of multi-object differentiation and we leave it for future work.

V. Remarks & Limitations

As the first attempt towards object distinguishing with off-the-shelf WLAN signals, TgaFree also possesses several limitations as follows.

LOS Requirement. In this paper, we only consider the LOS case and leave the NLOS case as our future work as aforementioned. It has to be admitted that LOS is a strict assumption in most realistic applications. Considering more robust applications in real life, the NLOS case needs to be paid much attention. Since different objects in NLOS shall also result in different propagation signatures, we expect that it is also feasible to recognize objects when they are placed in NLOS. Compared with LOS case, it is more challenging to recognize objects in NLOS since the propagation signatures are relatively minute. As a result, it requires more sophisticated extension of TagFree to accomplish this in our future work.

Object Category. In the present version of TagFree, we have only tested six categories of common objects. Considering the principle of TagFree, there exists a key restriction on objects to be distinguished. That is, objects must be different in at least one properties that have nonnegligible effect on signal propagation such as material, size and shape. Consequently, only those objects that can alter signal propagation notably that are probably to be distinguished by TagFree. It means that some small objects such as knife, pen and the like cannot be identified by TagFree at present. The limited number of objects restricts the broad application of TagFree in real life which is an issue to be further studied.

Object Location. Although we have considered the impact of location and proposed the concept of safe zone, the objects can not be distinguished accurately out of the safe zone centering around the location where the system is trained, which is due to the fact that radiometric signature is location-dependent. Moreover, for objects without approximate cylindrical symmetry such as Book and iPad, we have only considered its common orientation in our experiments. As a future work, exploring a more robust distinguishing scheme attracts our interest.

VI. Related Work

TagFree is related to the following categories of research.

Wireless Object and Device Identification. RFID systems are commonly adopted for wireless object identification, where a reader obtains information about an object via signals backscattered from a tag attached to the object [2], [22], [23]. TagFree is based on a similar identification procedure, yet directly differentiates objects by the signals "backscattered" by the object itself. This would potentially simplify backscatter based identification systems by eliminating the need for external tags. Some other methods have also been proposed for objects detection or identification using RF signals such as [24], [25], [26]. However, these methods all require sophisticated, expensive and bulky hardware equipment such as X-rays or ground penetrating radars. In terms of WiFi devices, both transient features (e.g. the envelope of the instantaneous amplitude [27]) and data features (e.g. modulation related frequency, magnitude and phase errors [28]) have been employed to uniquely identify WiFi network interface cards. TagFree also leverages the features extracted during radio communication, but identifies the objects along the propagation paths rather than the transceivers.

Wireless Device-free Human Localization/Detection. Device-free human localization systems locate a person by analyzing his impact on wireless signals received on pre-deployed monitors, while the person carries no wireless-enabled devices [7]. The underlying wireless infrastructure varies, including RFID [29][30], WiFi [3][7], ZigBee [31][32], etc., and the signal metrics range from coarse signal strength [7][32] to finer-grained PHY layer features [9][8]. Another scope of related work covers human events detection such as activities monitoring and gesture recognition using WiFi signals, specifically with CSI, such as [33], [34], [35], [36], [37]. However, TagFree leverages similar principles and also exploits the PHY layer features available on commercial WiFi devices [13], yet deviates from this thread of research in two aspects. 1) Most device-free systems assume the radiometric impact of each person is identical, while TagFree explores differentiable radio signatures for objects of distinct material, shapes and sizes. 2) Unlike most that correlate locations with received signals, we empirically figure out a *safe zone* where heterogeneity of objects, rather than locations, dominates the impact on radio propagation, and thus results in different received signal signatures.

VII. Conclusion

In this paper, we propose TagFree, a novel object differentiation scheme that leverages the unique radiometric properties of heterogeneous objects as their signatures. We further relax the correlation between location-dependent radiometric impact and object-specific radiometric impact, and propose the concept of *safe zone* to improve the robustness of TagFree. In addition, TagFree is able to differentiate multiple objects simultaneously via successive cancellation. Extensive experiments demonstrate that TagFree achieves up to 96% accuracy on distinguishing single object at the same location, and above 80% for safe zone range up to 3m along a 7m link. Moreover, TagFree can distinguish up to 3 objects simultaneously with reasonable accuracy. We have implemented TagFree on commercial WLAN infrastructure, and envision it as a practical solution that increases object distinguishing efficiency and reduces cost overhead for real-world deployment.

VIII. ACKNOWLEDGEMENTS

This research was supported in part by the China NSFC Grant 61472259, Shenzhen Science and Technology Foundation (No. KQCX20150324160536457), Guangdong Talent Project 2014TQ01X238, 2015TX01X111 and GDUPS (2015), Hong Kong RGC Grant HKUST16207714, Macao FDCT Grant 149/2016/A and the University of Macau Grant SRG2015-00050-FST.

978-1-5090-4327-9/17/$31.00 ©2017 IEEE

REFERENCES

[1] I. 15420:2009, "Information Technology - Automatic Tdentification and Data Capture Techniques - EAN/UPC Bar Code Symbology Specification."

[2] H. Vogt, "Efficient Object Identification with Passive RFID Tags," in *Proceedings of Springer-Verlag International Conference on Pervasive Computing*, 2002.

[3] A. E. Kosba, A. Saeed, and M. Youssef, "RASID: A Robust WLAN Device-free Passive Motion Detection System," in *Proceedings of IEEE PerCom*, 2012.

[4] J. Xiao, K. Wu, Y. Yi, L. Wang, and L. Ni, "FIMD: Fine-grained Device-free Motion Detection," in *Proceedings of IEEE ICPADS*, 2012.

[5] Z. Zhou, Z. Yang, C. Wu, L. Shangguan, and Y. Liu, "Towards Omnidirectional Passive Human Detection," in *Proceedings of IEEE INFOCOM*, 2013.

[6] F. Adib and D. Katabi, "See through walls with WiFi!" in *Proceedings of ACM SIGCOMM*, 2013.

[7] M. Youssef, M. Mah, and A. Agrawala, "Challenges: Device-free Passive Localization for Wireless Environments," in *Proceedings of ACM MobiCom*, 2007.

[8] J. Xiao, K. Wu, Y. Yi, L. Wang, and L. Ni, "Pilot: Passive Device-free Indoor Localization Using Channel State Information," in *Proceedings of IEEE ICDCS*, 2013.

[9] H. Abdel-Nasser, R. Samir, I. Sabek, and M. Youssef, "MonoPHY: Mono-Stream-based Device-free WLAN Localization via Physical Layer Information," in *Proceedings of IEEE Wireless Communications and Networking Conference*, 2013.

[10] Q. Pu, S. Gupta, S. Gollakota, and S. Patel, "Whole-Home Gesture Recognition using Wireless Signals," in *Proceedings of ACM MobiCom*, 2013.

[11] H. Abdelnasser, M. Youssef, and K. A. Harras, "Wigest: A ubiquitous wifi-based gesture recognition system," in *Proceedings of IEEE INFOCOM*, 2015, pp. 1472–1480.

[12] T. Rappaport, *Wireless Communications: Principles and Practice*, 2nd ed. Prentice Hall PTR, 2001.

[13] D. Halperin, W. Hu, A. Sheth, and D. Wetherall, "Predictable 802.11 Packet Delivery from Wireless Channel Measurements," in *Proceedings of ACM SIGCOMM*, 2010.

[14] D. Klair, K.-W. Chin, and R. Raad, "A Survey and Tutorial of RFID Anti-Collision Protocols," *IEEE Communications Surveys Tutorials*, vol. 12, no. 3, pp. 400–421, 2010.

[15] J. Wang, H. Hassanieh, D. Katabi, and P. Indyk, "Efficient and Reliable Low-power Backscatter Networks," in *Proceedings of ACM SIGCOMM*, 2012.

[16] C. Xu, B. Firner, R. S. Moore, Y. Zhang, W. Trappe, R. Howard, F. Zhang, and N. An, "SCPL: Indoor Device-free Multi-Subject Counting and Localization using Radio Signal Strength," in *Proceedings of ACM IPSN*, 2013.

[17] I. A. Gheyas and L. S. Smith, "Feature Subset Selection in Large Dimensionality Domains," *Pattern Recognition*, vol. 43, no. 1, pp. 5–13, 2010.

[18] I. Guyon and A. Elisseeff, "An Introduction to Variable and Feature Selection," *The Journal of Machine Learning Research*, vol. 3, pp. 1157–1182, 2003.

[19] M. Skurichina and R. P. W. Duin, "Bagging, Boosting and the Random Subspace Method for Linear Classifiers," *Pattern Analysis and Applications*, vol. 5, no. 2, pp. 121–135, 2002.

[20] T. K. Ho, "The Random Subspace Method for Constructing Decision Forests," *IEEE Transactions on Pattern Analysis and Machine Intelligence*, vol. 20, no. 8, pp. 832–844, 1998.

[21] D. Cai, X. He, and J. Han, "SRDA: An Efficient Algorithm for Large-Scale Discriminant Analysis," *IEEE Transactions on Knowledge and Data Engineering*, vol. 20, no. 1, pp. 1–12, 2008.

[22] T. Li, S. Chen, and Y. Ling, "Identifying the Missing Tags in a Large RFID System," in *Proceedings of ACM MobiHoc*, 2010.

[23] L. Xie, B. Sheng, C. Tan, H. Han, Q. Li, and D. Chen, "Efficient Tag Identification in Mobile RFID Systems," in *Proceedings of IEEE INFOCOM*, 2010.

[24] L. L. Monte, D. Erricolo, F. Soldovieri, and M. C. Wicks, "Radio frequency tomography for tunnel detection," *IEEE Transactions on Geoscience and Remote Sensing*, vol. 48, no. 3, pp. 1128–1137, 2010.

[25] K. D. Krug, W. F. Aitkenhead, R. F. Eilbert, J. H. Stillson, and J. A. Stein, "Detecting explosives or other contraband by employing transmitted and scattered x-rays," Feb. 4 1997, US Patent 5,600,700.

[26] K. D. Krug, J. O. Tortora, R. Bijjani, and R. F. Eilbert, "Multiview x-ray based system for detecting contraband such as in baggage," Jul. 11 2000, US Patent 6,088,423.

[27] O. Ureten and N. Serinken, "Wireless Security through RF Fingerprinting," *Canadian Journal of Electrical and Computer Engineering*, vol. 32, no. 1, pp. 27–33, 2007.

[28] V. Brik, S. Banerjee, M. Gruteser, and S. Oh, "Wireless Device Identification with Radiometric Signatures," in *Proceedings of ACM MobiCom*, 2008.

[29] Y. Liu, Y. Zhao, L. Chen, J. Pei, and J. Han, "Mining Frequent Trajectory Patterns for Activity Monitoring Using Radio Frequency Tag Arrays," *IEEE Transactions on Parallel and Distributed Systems*, vol. 23, no. 11, pp. 2138–2149, 2012.

[30] D. Zhang, J. Zhou, M. Guo, J. Cao, and T. Li, "TASA: Tag-Free Activity Sensing Using RFID Tag Arrays," *IEEE Transactions on Parallel and Distributed Systems*, vol. 22, no. 4, pp. 558–570, 2011.

[31] D. Zhang, J. Ma, Q. Chen, and L. M. Ni, "An RF-Based System for Tracking Transceiver-Free Objects," in *Proceedings of IEEE PerCom*, 2007.

[32] J. Wilson and N. Patwari, "Radio Tomographic Imaging with Wireless Networks," *IEEE Transactions on Mobile Computing*, vol. 9, no. 5, pp. 621–632, 2010.

[33] C. Han, K. Wu, Y. Wang, and L. M. Ni, "Wifall: Device-free fall detection by wireless networks," in *Proceedings of IEEE INFOCOM*, 2014, pp. 271–279.

[34] Y. Wang, J. Liu, Y. Chen, M. Gruteser, J. Yang, and H. Liu, "E-eyes: device-free location-oriented activity identification using fine-grained wifi signatures," in *Proceedings of ACM Mobicom*, 2014, pp. 617–628.

[35] G. Wang, Y. Zou, Z. Zhou, K. Wu, and L. M. Ni, "We can hear you with wi-fi!" in *Proceedings of ACM Mobicom*, 2014, pp. 593–604.

[36] X. Liu, J. Cao, S. Tang, and J. Wen, "Wi-sleep: Contactless sleep monitoring via wifi signals," in *Proceedings of IEEE RTSS*, 2014, pp. 346–355.

[37] K. Ali, A. X. Liu, W. Wang, and M. Shahzad, "Keystroke recognition using wifi signals," in *Proceedings of ACM Mobicom*, 2015, pp. 90–102.

978-1-5090-4327-9/17/$31.00 ©2017 IEEE